Population pharmacokinetic model of irinotecan and its four main metabolites in patients treated with FOLFIRI or FOLFIRINOX regimen

Laure Deyme, Dominique Barbolosi, Litaty Céphanoée Mbatchi, Nicole Tubiana-Mathieu, Marc Ychou, Alexandre Evrard, Florence Gattacceca

Title: Population pharmacokinetic model of irinotecan and its four main metabolites in patients treated with FOLFIRI or FOLFIRINOX regimen

Authors: Laure Deyme[1], Dominique Barbolosi[1], Litaty Céphanoée Mbatchi[2,3], Nicole Tubiana-Mathieu[4], Marc Ychou[5], Alexandre Evrard[2,3], and Florence Gattacceca[1]

Affiliations:
1 SMARTc, Centre de Recherche en Cancérologie de Marseille (CRCM), INSERM U1068, CNRS UMR 7258, Aix-Marseille Université and Institut Paoli-Calmettes, Faculté de Pharmacie, Marseille, France.
2 Laboratoire de Biochimie et Biologie Moléculaire, CHU Nîmes-Carémeau, Nîmes, France.
3 IRCM, Inserm U1194, Université de Montpellier, Montpellier, France.
4 Centre Hospitalier Universitaire de Limoges, Limoges, France.
5 Institut Régional du cancer de Montpellier (ICM)-Val d'Aurelle, Montpellier, France.

Corresponding author:
Laure Deyme,
E-mail adress: laure.deyme@gmail.com
Telephone number: +33 4 91 83 55 09

ORCID numbers:
L Deyme 0000-0002-5986-4765
F Gattacceca 0000-0002-4944-8063

Keywords: CPT-11, FOLFIRI, FOLFIRINOX, Population pharmacokinetics, Nonlinear mixed effect modelling

Declarations

Funding information: This work was supported by a Grant from Cancéropôle Grand Sud-Ouest (France).

Conflict of Interest statement: Laure Deyme, Dominique Barbolosi, Litaty Céphanoée Mbatchi, Nicole Tubiana-Mathieu, Marc Ychou, Alexandre Evrard, and Florence Gattacceca declare that they have no conflict of interest.

Ethics approval: All procedures performed in studies involving human participants were in accordance with the ethical standards of the institutional and/or national research committee and with the 1964 Helsinki Declaration and its later amendments or comparable ethical standards.

Informed consent: Informed consent was obtained from all individual participants included in the study.

Data availability: The datasets generated and analyzed during the current study are available from the corresponding author on reasonable request.

Code availability: The model code that we developed is provided as an electronic supplementary information, so the model can be copy-pasted by any reader and run directly on Monolix® software with the users' own dataset.

Abstract

Purpose: The aim of the present study was to characterize the pharmacokinetics of irinotecan and its four main metabolites (SN-38, SN-38G, APC and NPC) in metastatic colorectal cancer patients treated with FOLFIRI and FOLFIRINOX regimens and to quantify and explain the inter-individual pharmacokinetic variability in this context.

Methods: A multicenter study including 109 metastatic colorectal cancer patients treated with FOLFIRI or FOLFIRINOX regimen, associated or not with a monoclonal antibody, was conducted. Concentrations of irinotecan and its four main metabolites were measured in 506 blood samples during the first cycle of treatment. Collected data were analyzed using the population approach. First, fixed and random effects models were selected using statistical and graphical methods; second, the impact of covariates on pharmacokinetic parameters was evaluated in order to explain the inter-individual variability in pharmacokinetic parameters.

Results: A seven-compartment model best described the pharmacokinetics of irinotecan and its four main metabolites. First-order rates were assigned to distribution, elimination, and metabolism processes, except for the transformation of irinotecan to NPC which was nonlinear. Addition of a direct conversion of NPC into SN-38 significantly improved the model. Co-administration of oxaliplatin significantly modified the distribution of SN-38.

Conclusion: To our knowledge, the present model is the first to allow a simultaneous description of irinotecan pharmacokinetics and of its four main metabolites. Moreover, a direct conversion of NPC into SN-38 had never been described before in a population pharmacokinetic model of irinotecan. The model will be useful to develop pharmacokinetic-pharmacodynamic models relating SN-38 concentrations to efficacy and digestive toxicities.

Clinical trials registration number: ClinicalTrials.gov identifier: NCT00559676

1. Introduction

Irinotecan (CPT-11) is a semisynthetic derivative of camptothecin used as an anticancer drug in various solid tumors since the 1990s. CPT-11 is a treatment for patients with metastatic colorectal cancer and pancreatic cancer, used in combination with leucoverin, 5-fluorouracil (FOLFIRI) and oxaliplatin (FOLFIRINOX) with or without a monoclonal antibody as bevacizumab or cetuximab. In both regimens, CPT-11 dose is 180 mg/m2 administrated as an intravenous (IV) infusion over 90 min.

Dose-limiting digestive toxicities are frequently described when using CPT-11 alone or in combination. CPT-11 effects display a large interindividual variability (IIV), which mostly originates from variations in the dose-exposure relationship. Indeed, CPT-11 displays a highly complex metabolism, involving various phase I and II enzymes and making exposure to CPT-11 and its metabolites prone to environmental and genetic influences. A better characterization of the pharmacokinetic (PK) IIV of CPT-11 and its metabolites is consequently warranted to individualize dosing regimens and prevent excessive toxicities while maintaining the efficacy [1].

CPT-11 is a prodrug which is metabolized by liver carboxylesterases into a more cytotoxic form, SN-38 (7-Ethyl-10-hydroxy-camptothecin), and by liver cytochromes P450 (CYP) 3A4/5 into two inactive forms, APC (7-ethyl-10-[4-N-(5-aminopentanoicacid)-1-piperidino] carbonyloxycamptothecin) and NPC (7-ethyl-10-[4-(1-piperidino)-1-amino]-carbonyloxycamptothecin). SN-38 is detoxified by UDP glucuronosyltransferase family 1 member A1 (UGT1A1) into SN-38G (glucuronidated SN-38), an inactive metabolite, before biliary excretion [1]. A rebound peak was frequently observed in SN-38 PK [1–8] which has been ascribed to an enterohepatic recirculation (HER) [6] or to a release from erythrocytes [7]. The mechanism of action of CPT-11 and SN-38 consists in inhibiting topoisomerase I and causing double-strand DNA breakage, which conducts to cell death [9].

Various kinds of transporters and enzymes are involved in the metabolic biotransformation and elimination of CPT-11 and SN-38, which partly explains the large pharmacokinetic (PK) inter-individual variability. Among these transporters, the ABC transporter family is highly implicated. UGT1A1 activity is highly variable between individuals, which can be due to TATA box polymorphism of the UGT1A1 promoter region that impact the SN-38 PK and subsequently CPT-11 efficiency and toxicity[8]. In Caucasians, the most frequent TATA box polymorphism is on the UGT1A1*28 allele and the number of TA repeats for this allele is six or seven. The number of TA repeats is inversely proportional to UGT1A1 transcription and thus to UGT1A1 enzyme activity. *ABCB1* and *CYP3A4* genes are regulated by a transcriptional factor, the nuclear receptor subfamily 1, group I, member 2 (NR1I2), also named pregnane X receptor (PXR)[9].

Population pharmacokinetic (PopPK) models use data from all subjects simultaneously to describe the concentration-time profile of a drug and its interindividual variability. Seven CPT-11 PopPK models have been published so far, between 2002 and 2019, with an increasingly detailed description of the PK over time [2,10,11]. Among them, Poujol et al model [12] concerns patients with digestive cancer treated with FOLFIRI; Oyaga-Iriarte et al [2] model describes the PK of CPT-11, SN-38 and SN-38G in metastatic colorectal cancer patients treated with FOLFIRINOX. However, no model including NPC metabolite was developed until now. Including data from an additional metabolite compartment should help describing the PK of SN-38 with more precision.

With the objective to provide an accurate model for dosing optimization, the present study aimed to describe the PK of CPT-11 and its four main metabolites (SN-38, SN-38G, APC and NPC) in metastatic colorectal cancer patients treated with FOLFIRI and FOLFIRINOX regimens and to quantify and explain the inter-individual PK variability in this context.

2. Patients and methods

2.1. Patients and study design

PK data were available in 109 of the 200 metastatic colorectal cancer patients included in the BIO-COLON multicentric phase IV study (ClinicalTrials.gov identifier: NCT00559676) [13]. This trial was approved by the Ethical Committee of Dupuytren University Hospital (Limoges, France) and all participants provided a written informed consent before enrollment in the study. The main eligibility criteria were a World Health Organization performance status between 0 and 2 and histologically confirmed metastatic colorectal cancer. All patients in the PK study received an irinotecan-based chemotherapy regimen like FOLFIRI or FOLFIRINOX in association or not with a monoclonal antibody: bevacizumab or cetuximab. In all cases, the standard dose of CPT-11 was 180 mg/m² by IV infusion over 90 min.

Plasma samples were collected at five different times during the first cycle of treatment, namely 1.5, 4.5, 7.5, 28.5, and 46 h after the beginning of the infusion. Plasma concentrations of CPT-11 and its four metabolites were measured by high-performance liquid chromatography-fluorescence method [14]. The lower limit of quantification (LOQ) for that method was 0.5 µg/L for irinotecan and its four metabolites, which corresponds to 0.85 nmol/L for CPT-11, 1.27 nmol/L for SN-38, 0.879 nmol/L for SN-38G, 0.808 nmol/L for APC and 0.964 nmol/L for NPC according to their respective molar mass. 505 plasma samples from 109 metastatic colorectal cancer patients (69 males and 40 females) were available for analysis. Data collected for each patient were: sex, body surface area (BSA), weight, height, treatment regimen, performance status prior cycle 1, TATA box polymorphism of the UGT1A1 promoter region and NR1I2-rs10934498 polymorphism.

2.2. Population pharmacokinetic analysis

The PopPK analysis of CPT-11 and its four metabolites was performed using the nonlinear mixed-effect modelling approach with Monolix® software version 2019R1 (Lixoft, Anthony, France, http://lixoft.com/). The algorithm implemented in Monolix® for population parameter estimation is the stochastic approximation expectation-maximization (SAEM) algorithm. Data below the LOQ (BLOQ) were considered as left-censored observations (density function goes from LOQ to negative infinity). In the dataset, time was expressed in hours (h), doses in micromoles (µmol) and concentrations in micromoles per liter (µM).

The structural identifiability of the full model (parent and metabolite molecules) was tested by exploring the rank of the sensitivity matrix by the derivative-based local method using MatlabR2019b® software (The MathWorks Inc, Natick, Massachusetts) [15]. Parameter reduction was performed to ensure structural identifiability when needed, by combining rate constants and using metabolism fractions and apparent volumes of distribution. When parameters were poorly estimated in the model, they were fixed to an optimal plausible value determined by a parameter sensitivity analysis.

Based on previously published models and visual inspection of the data, one-, two- and three-compartment models were tested with linear, Michaelis-Menten or mixed elimination for each molecule. The structural PK model was built gradually from CPT-11 to metabolites:

- Select the CPT-11 structural model and estimate PK parameters
- Use CPT-11 individual parameters to select the APC structural model and to estimate PK parameters
- Set the APC fixed effects in the model, to select the NPC structural model and to estimate PK parameters
- Set the NPC fixed effects in the model, to select SN-38 and SN-38G structural models and to estimate PK parameters
- Estimation of all PK parameters simultaneously combining the selected structural models.

The individual PK parameters were assumed lognormally distributed, except f_a which represents a proportion and was assumed to follow a probit distribution. Additive, proportional and combined error models were tested to describe the residual variability of each molecule.

Several models were tested to account for the rebound of SN-38 PK (Fig. 1):

a) delayed differential equation
b) gallbladder compartment with a delayed return to SN-38 central compartment
c) gallbladder compartment with a delayed return to SN-38 peripheral compartment
d) double transformation of CPT-11 into SN-38, one of whom with a delay
e) reconversion of NPC into SN-38 with or without delay
f) reconversion of SN-38G into SN-38 with or without delay.

In models a, b, c, EHR of SN-38 was assumed and modelled by introducing either a delayed differential equation with a constant delay applied to the central compartment of SN-38, or a gallbladder compartment as proposed by Gabrielsson et al [16]. In models d, e, f, conversion of another metabolite into SN-38 was assumed to explain the rebound.

Once the structural and statistical models were selected, the covariate model was built. The impact of the following covariates was tested on each PK parameter: body surface area (BSA), height, weight, gender, regimen, association with antibody, performance status and UGT1A1*28 polymorphism. Continuous covariates (BSA, weight and height) were centred to the population median values. Various allocations to subgroups were tested for non-dichotomous categorical covariates. *NR1I2-rs10934498* polymorphism was not tested in covariate analysis because the information was missing in 15 patients. To spare calculation time, a pre-selection of relevant covariates was performed before inclusion in the model based on the likelihood ratio test. As a first step, a principal component analysis was performed using the 'pca' function implemented in MatlabR2019b® software to select the most informative continuous covariates. Then, a screening of influential covariates was performed from probability density functions using indexes derived from information theory [17] and calculations were performed with MatlabR2019b® software. Briefly, for each covariate, indexes are based on the concept of negative entropy and quantify the amount of information brought by the covariate to the distribution of a given PK parameter. Next, covariates were included one by one in the popPK model, in decreasing order of the amount of information. This inclusion phase ended when the objective function value (OFV), which corresponds to the value of -2 Log Likelihood (-2LL), stopped decreasing, i.e., when the decrease in OFV was smaller than 7.88 when adding one parameter, which corresponds

to a negative likelihood ratio test at the 0.5% significance level. In addition to its statistical significance, a covariate was selected if the following conditions were fulfilled: good precision of the parameter estimates, acceptable residual errors, decreased unexplained inter-individual variability of the PK parameter related to the covariate.

Model selection and evaluation were performed based on numerical criteria, such as values of OFV for nested models and Akaike information criteria (AIC) otherwise, relative standard errors (RSE) and residual errors, and on graphical assessment using Goodness-of-fit (GOF) plots and visual predictive checks (VPC).

3. Results

3.1. Patients

Nineteen patients were treated with FOLFIRINOX regimen, 87 with FOLFIRI regimen and three with one or another chemotherapy regimen. 63 patients received in addition one monoclonal antibody (cetuximab for three patients and bevacizumab for 60 patients). The baseline characteristics of patients are summarized in Table 1.

Number of patients	**109**
Number of samples	505
Number of plasma concentrations	2,524
BSA (median [range]) (m^2)	1.78 [1.38 - 2.2]
Weight (median [range]) (kg)	68 [41 - 109]
Height (median [range]) (cm)	169 [145 – 190]
Sex	
Female	40
Male	69
Regimen	
FOLFIRI	87
FOLFIRINOX	19
Unknown	3
+ Monoclonal Ab	63
Bevacizumab	*60*
Cetuximab	*3*
Performance Status	
0	63
1	37
2	9
UGT1A1*28	
$(TA)_6/(TA)_6$	46
$(TA)_7/(TA)_6$	45
$(TA)_7/(TA)_7$	11
Unknown	7
NR1I2 – rs10934498	
AA	23
AG	45
GG	26
Unknown	15

Table 1: Patient characteristics.
Values represent number of patients unless otherwise stated. **BSA:** body surface area; + **monoclonal Ab:** associated with monoclonal antibody; **UGT1A1*28:** TATA box polymorphism of the UGT1A1 promoter region; **NR1I2 – rs10934498:** NR1I2-rs10934498 polymorphism

3.2. Pharmacokinetic analysis

A total of 2,525 plasma concentrations (505 observations for each molecule) were available for analysis, among which one SN-38 and six NPC concentrations reported as below LOQ (BLOQ) were left-censored. At the beginning of the analysis, one atypical sample at 5.5 hour was removed: indeed, a sample stability problem was assumed since concentrations of CPT-11 and its four main metabolites were inconsistently low, 0.163 µmol/L for CPT-11, with respect to prior (5.38 hour) and following (6.63 hour) samples for the same patient, with 1.92 and 1.36 µmol/L for CPT-11 respectively.

The data of CPT-11 and its four main metabolites were described by a seven-compartment model (Fig. 2). CPT-11 PK was best described by a 2-compartment model. Two compartments were also required for SN-38. Observed kinetic profiles of SN-38G, APC and NPC metabolites were described by a 1-compartment model. SN-38 metabolite was eliminated from the system by transformation into SN-38G (k_{35}).

For structural identifiability requirements, the elimination rate constant of CPT-11 (k_1) and the metabolism rates of CPT-11 to SN-38 (k_{13}) and to APC (k_{16}) were combined together in one unique parameter denoted k_e as follows:

$$k_e = k_1 + k_{13} + k_{16}.$$

By using k_e and the metabolism fractions f_3 andf_6 associated with the metabolism of CPT-11 into SN-38 and APC, respectively, we obtained:

$$k_{13} = f_3 k_e \quad ; k_{16} = f_6 k_e$$

for the metabolism rates k_{13} andk_{16}, respectively. Consequence of this re-parameterization is the scaling of V_3, V_5 and V_6 volumes of distribution for SN-38, SN-38G and APC, respectively, which became apparent volumes (respectively V_{3a}, V_{5a} and V_{6a})

$$\mathrm{V}_{3a} = \frac{\mathrm{V}_3}{f_3} \quad ; \quad \mathrm{V}_{5a} = \frac{\mathrm{V}_5}{f_3} \quad ; \quad \mathrm{V}_{6a} = \frac{\mathrm{V}_6}{f_6}.$$

The model using these apparent volumes became structurally identifiable.

The conversion from CPT-11 into NPC was best described with a Michaelis-Menten equation, involving V_{max} and K_m parameters. Elimination of SN-38G, APC and NPC were of first order, with k_5, k_6 and k_7 rate constants, respectively.

A rebound was observed in SN-38 PK of many patients around 8 hours (Fig. 3f). This rebound was best described by a reconversion of NPC into SN-38 with a delay differential equation by the term:

$$k_7 * f_a * \frac{V_7}{V_{3a}} * C_7(\mathrm{t} - \tau)$$

involving the delay (τ).

The fraction of NPC to be converted to SN-38 (f_{ehr}) was considered as a part of NPC elimination constant (k_7). Since V_{3a} is an apparent volume of distribution, this fraction must be divided by f_3 to obtain a single parameter (f_a) as follows:

$$f_a = \frac{f_{ehr}}{f_3}$$

Residual error was best described by a proportional error model for CPT-11, SN-38, SN-38G and APC, whereas a combined error model (combination of additional and proportional terms) performed better for NPC.

Due to the sparseness of the data and the large number of parameters, some model parameters could not be accurately estimated and were either removed, such as the IIV of k_{21},V_{3a}, V_{max} and K_m, or fixed, such as the typical value of V_{max} and the IIV of k_e. To select the best fixed value, a sensitivity analysis was performed by testing several plausible values from which the one with the lowest OFV was retained, provided the model was stable for the values in the same range. For example, to fix the typical value of V_{max}, seven values were tested (0.050, 0.10, 0.20, 0.25, 0.30, 0.35 and 0.4): the value of 0.30 µmol. L^{-1} resulted in the lowest OFV and was consequently retained.

PK parameters followed a lognormal distribution with two exceptions. k_e was assumed to follow a normal distribution based on the observation of the empirical distribution of the individual parameters, which allowed to decrease OFV. f_a represents a proportion and was assumed to follow a probit distribution.

The code of the final model is provided in Supplementary file 1. The values of the popPK parameters of the base model (without covariate) and of the final model (with covariates) are provided in Table 2.

	Model without covariate		**Final model**	
	VALUE (RSE%)			
	Fixed effect	**ω**	**Fixed effect**	**ω**
V_1 (L)	91 (3.82)	0.344 (7.93)	94.6 (3.92)	0.353 (8.37)
V_{3a} (L)	91.1 (2.72)	-	97.4 (6.40)	-
V_{5a} (L)	57.6 (6.22)	0.441 (8.26)	41.6 (5.14)	0.285 (15.1)
β_{V5a_PS2}	-	-	*- 0.52 (25.5)*	-
V_{6a} (L)	173 (8.31)	0.804 (7.74)	209 (9.75)	0.698 (8.11)
β_{V6a_Female}	-	-	*- 0.447 (34.3)*	-
β_{V6a_Weight}	-	-	*1**	-
β_{V6a_PS2}	-	-	*- 0.797 (32.6)*	-
V_7 (L)	154 (7.5)	0.691 (7.89)	173 (8.41)	0.59 (7.67)
β_{V7_Female}	-	-	*- 0.427 (32.6)*	-
β_{V7_Weight}	-	-	*1**	-
k_e (h^{-1})	0.171 (4.07)	0.05*	0.164 (3.88)	0.05*

k_{12} (h^{-1})	0.186 (4.77)	0.284 (10.2)	0.17 (4.7)	0.268 (10.7)
k_{21} (h^{-1})	0.133 (3.49)	-	0.128 (3.45)	-
V_{max} ($\mu mol.h^{-1}$)	0.3*	-	0.3*	-
K_m ($\mu mol.L^{-1}$)	3.23 (5.01)	-	3.39 (5.91)	-
k_{34} (h^{-1})	6.55 (10.6)	0.942 (8.68)	7.23 (10.4)	0.851 (8.48)
k_{43} (h^{-1})	0.0214 (7.62)	0.396 (14.2)	0.0143 (7.73)	0.413 (18.2)
$\beta_{k43\_FOLFIRINOX}$	-	-	*- 0.855 (20)*	-
k_{35} (h^{-1})	4.13 (5.63)	0.427 (9.17)	3.33 (7.82)	0.243 (16.8)
$\beta_{k35\_UGT\_6/7}$	-	-	*- 0.41 (18.5)*	-
$\beta_{k35\_UGT\_7/7}$	-	-	*- 1.02 (13)*	-
k_5 (h^{-1})	1.39 (4.27)	0.29 (13.7)	1.29 (4.14)	0.24 (19.4)
k_6 (h^{-1})	0.406 (5.03)	0.441 (8.96)	0.422 (4.94)	0.425 (9.24)
β_{k6_Weight}	-	-	*- 0.921 (25.7)*	-
k_7 (h^{-1})	1.27 (5.59)	0.458 (10.5)	1.49 (7.62)	0.488 (10.4)
β_{k7_tPS1-2}	-	-	*- 0.298 (37.6)*	-
τ (h)	6.44 (12.2)	0.786 (12.5)	8.38 (8.82)	0.581 (13.3)
f_a	0.81 (7.55)	0.665 (20.1)	0.89 (4.47)	0.688 (45)
b_1 (%)	22.7 (4.3)		22.5 (4.4)	
b_3 (%)	21.9 (4.72)		22.2 (4.77)	
b_5 (%)	19.9 (4.98)		20.8 (4.98)	
b_6 (%)	19.1 (4.77)		19.5 (5.12)	
a_7 ($nmol.L^{-1}$)	0.925 (8.92)		0.938 (8.77)	
b_7 (%)	15.4 (6.84)		14.8 (6.84)	
OFV (-2LL)	**-10,732**		**-10,881**	
AIC	**-10,658**		**-10,791**	

Table 2: Population pharmacokinetic parameters of irinotecan and its four main metabolites from the 7-compartment model without and with covariates. Estimations from the data from 102 patients displaying UGT1A1 status.

V_1: volume of the central compartment for CPT-11, **k_{12}**: rate constant from central compartment of CPT-11 to peripheral compartment of CPT-11 ; **k_{21}**: rate constant from peripheral compartment of CPT-11 to central compartment of CPT-11 ; **k_1**: elimination rate of CPT-11, **k_{13}**: metabolism rate of CPT-11 into SN-38, **k_{16}**: metabolism rate of CPT-11 into APC; **k_e**: combination of k_1, k_{13} and k_{16}; **V_{max}**: maximum rate of metabolism of CPT-11 into NPC; **K_m**: the half-saturating concentration of CPT-11 for metabolism of CPT-11 into NPC; **V_{3a}:** apparent volume of the central compartment for SN-38, **k_{34}**: rate constant from central compartment of SN-38 to peripheral compartment of SN-38; **k_{43}**: rate constant from peripheral compartment of SN-38 to central compartment of SN-38 ; **k_{35}**: metabolism rate of SN-38 into SN-38G; **V_{5a}**: apparent volume of the central compartment for SN-38G; **k_5**: elimination rate of SN-38G; **V_{6a}**: apparent volume of the central compartment for APC; **k_6**: elimination rate of APC; **V_7**: Volume of the central compartment for NPC; **r**: ratio of metabolism rate of NPC into SN-38 on metabolism fraction of CPT-11 into SN-38; **τ**: delay; **k_7**: elimination rate of NPC; **$\beta_{parameter\_covariate}$**: effect value of covariate on the parameter; **ω**: standard deviation of random effect; **b_1**: proportional residual error for CPT-11; **b_3**: proportional residual error for SN-38; **b_5**: proportional residual error for SN-38G; **b_6**: proportional residual error for APC; **a_7**: constant residual error for NPC; **b_7**: proportional residual error for NPC; *****: fixed value; **OFV**: objective function value; **-2LL**: - 2 Log Likelihood; **AIC**: Akaike information criteria; **-**: not included in the model

As UGT1A1 status was unknown for 7 patients, the covariate model was developed from 102 patients only. Anyway, the parameter estimates obtained with the base model without covariate were similar for the reduced dataset with 102 patients and the initial dataset with 109 patients. Based on

the information tool, the most relevant covariate effect was the TATA box polymorphism of the UGT1A1 promoter region on the transformation rate from SN-38 into SN-38G, k_{35}, which was included in the model using the following equation:

$$k_{35}(\mathrm{i}) = \mathrm{k}_{35} * e^{cov\_UGT\ (i)} * e^{\eta_{k35}(i)}$$

with k_{35} the typical value for the reference population of homozygous wild-type $(TA)_6/(TA)_6$ patients, cov_UGT equal to $\beta_{k35\_UGT\_6/7}$ for heterozygous mutant-type $(TA)_6/(TA)_7$ patients, or to $\beta_{k35\_UGT\_7/7}$ for homozygous mutant-type $(TA)_7/(TA)_7$ patients. Inclusion of this categorical covariate led to a decrease of 13.7% of the IIV of k_{35} (25.6% vs 39.3%) and a drop of 54 points of the OFV.

To assess the regimen covariate, 3 patients, whose chemotherapy regimen was uncertain, were recorded as belonging to the dominant group: FOLFIRI. The chemotherapy regimen was included as binary covariate in the model using the following equation:

$$k_{43}(i) = k_{43} * e^{cov\_REGIMEN(i)} * e^{\eta_{k43}(i)}$$

with $cov\_REGIMEN$ equal to null for patients treated with FOLFIRI or to $\beta_{43\_FOLFIRINOX}$ for patients trea ted with FOLFIRINOX. The effect of co-administration of oxaliplatin was significant on k_{43} and decrea sed the IIV of k_{43} of 6.2% (36.9% vs 43.1%) and dropped the OFV of 20 points, which suggests a PK int eraction between oxaliplatin and SN-38. Contrarily, co-administration of antibody, bevacizumab or ce tuximab, was not a significant covariate.

The principal component analysis revealed that BSA was included in the height and weight. BSA was no longer studied and height and weight were considered as the only size covariates. These continuous covariates were included in the model using the following equation:

$$\theta(i) = \theta * \left(\frac{weight(i)}{68}\right)^{\beta} * e^{\eta_\theta(i)}$$

with β fixed at 1 to describe a linear relationship (β_{V6a_Weight} and β_{V7_Weight}).

Weight was retained as covariate on V_{6a}, V_7 and k_6 in the final model. A linear relationship between weight and V_{6a} and V_7 parameters was found to significantly improve the model: the OFV decreased of 13 and 16 points, respectively. A power relationship between weight and $\boldsymbol{k}_6$ was also significant and led to a 9 point-drop of the OFV.

Concerning performance status, two different group allocation strategies were used to create two subgroups:

- PS: the reference subgroup includes patients with a performance status of 0 or 1
- tPS: the reference subgroup includes patients with a performance status of 0.

PS was retained as covariate on V_{5a} and V_{6a} and tPS on k_7. These binary covariates allowed to decrease the OFV of 8.4, 11 and 10 points, respectively.

Gender was also included as a binary covariate in the final model on V_{6a} and V_7. This inclusion decreased the OFV of 13 and 15 points, respectively. No other effect of covariates on PK parameters was found significant.

Numerical criteria showed the robustness of the final model. Parameters were estimated with a good precision, with RSE <30%, except for $\omega(f_a)$ (47.1%). Values of residual errors were acceptable,

with a maximum of 22.5% for CPT-11 (Table 2). Addition of relevant covariates allowed to explain the PK IIV of CPT-11 and its four main metabolites.

Performance of the final model was further assessed by evaluating GOF plots of SN-38 (Fig. 3), which accounts for the major part of CPT-11 treatment activity. The conditional weighted residuals of SN-38 were normally distributed (Fig. 3b and c). The population and individual predictions of SN-38, the active metabolite, were uniformly distributed around the line of unity (Fig. 3d and e). Additional GOF plots for CPT-11 and metabolites, including normalized prediction distribution errors, are provided in Supplementary file 2 and showed similar patterns.

VPC were performed for each molecule by comparing 500 datasets simulated from the final parameters with the observed concentrations (Fig. 4 for SN-38, supplementary file 2 for other molecules) and showed a satisfactory prediction of the typical profile and of the associated variability.

4. Discussion

Our study allowed the development of a robust model with a good quality of predictions and inclusion of significant covariates. To the best of our knowledge, we developed the first PopPK model simultaneously describing the PK of CPT-11 and four of its main metabolites, SN-38, SN-38G, APC and NPC. Indeed, NPC PK had never been explored before, and this additional information proved essential for a proper characterization of the rebound of SN-38 and SN-38G PK. Moreover, the PK of CPT-11 and its active metabolite SN-38 was characterized for the first time in a population containing both FOLFIRI- and FOLFIRINOX-treated patients, allowing to assess the impact of oxaliplatin on the PK of CPT-11 and metabolites. Indeed, seven references reported PopPK studies of CPT-11 so far [2,10,11,14,18–21]. In all studies, but Kimura et al. [21], PK of SN-38 was studied in addition to PK of CPT-11. Four studies additionally included PK of SN-38G [2,11,18–20], among which two also assessed PK of APC [18,20]. Four studies described the PK of CPT-11 and metabolites in patients treated for various solid tumors with irinotecan as a single agent: two studies were conducted in a paediatric population [20,21], Berg et al. assessed the impact of co-medication by enzyme-inducing antiepileptic drugs and corticosteroids [18] and Klein et al. also included patients suffering from lymphoma [19]. Only two studies were performed in a similar context to the present study, *ie* in populations of digestive cancer patients treated either with FOLFIRI [12] or FOLFIRINOX [2].

The structural model which best described PK of CPT-11 in our study was a 2-compartment model, consistently with most previous studies [18,20]. PK of SN-38 and SN-38G were best described by a 2-compartment and a 1-compartment model, respectively, in line with all previously published models, except in Oyaga-Iriarte et al. [2] where a 1-compartment model was reported for SN-38 and a 2-compartment model for SN-38G. Finally, APC was best described with a 1-compartment model, consistently with Thompson et al. [20] although a 2-compartment model had been described in Berg et al. [18]. The differences between the studies might arise from the amount of data available to describe the rapid decay phase of the 2-comparment model.

Our model is the first to propose a physiologically relevant description of the rebound of SN-38 and SN-38G, through a reconversion of NPC into SN-38 with delay, which was made possible by the inclusion of NPC PK. This model is consistent with the mechanistic knowledge about pharmacology of CPT-11 and metabolites, since it has been shown that NPC can be transformed into SN-38 by carboxylesterases 1 and 2 [22]. Moreover, to the best of our knowledge, the present work is the first example of the use of delay differential equations to describe EHR. Oyaga-Iriarte et al. [2] recently

included an enterohepatic cycle, described by a single-direction flow from SN-38G peripheral compartment to the SN-38 compartment. The model of Oyaga-Iriarte et al.[4] also considered that CPT-11 was totally transformed into SN-38, while we considered that CPT-11 was metabolized into SN-38, SN-38G, APC and NPC and could additionally be eliminated directly, which is more relevant physiologically.

Parameter estimates were compared to previously published models. Oyaga-Iriarte et al. publication [2] was excluded from parameter comparison since the assumption that CPT-11 was totally transformed into SN-38 was too different from ours. When needed for comparison, elimination clearances, inter-compartmental clearances and peripheral volumes were calculated from transfer constants and volumes from the following formulas:

$$Cl_i = V_i * k_i \text{ and } Q_i = V_i * k_{ij} = V_j * k_{ji}$$

Parameter estimates were in the same range as previously published values. Differences between the various studies might arise from the characteristics of the populations studied, but also to the number of compartments in the models. Indeed, a lower value of the volume of distribution can be obtained through a better description of the distribution with additional distribution compartments. Steady state volume of distribution of CPT-11 was 226.7 L, similar to those reported in published models, comprised between 140.4 and 300L [10,11]. The inclusion of NPC PK led us to add a non-linear component in CPT-11 elimination: with a clearance of 15.0 L/h, our linear elimination was accordingly lower than reported linear clearances, comprised between 16.9 and 43.8 L/h. The apparent central volume of distribution of SN-38 (79.8 L) was slightly lower and the peripheral volume of distribution of SN-38 (54,325 L) was similar to published parameters, comprised between 132.7 and 408 L and between 4,916 and 71,600 L respectively. The intercompartmental clearance and the clearance of SN-38 were respectively of 706 L/h and 247 L/h, in line with those previously reported. The apparent volume of distribution (187 L) and the elimination constant rate of APC (0.444 h^{-1}) are very close to those previously reported, respectively between 232 and 379 L and between 0.54 and 0.59 h^{-1}. Proportional residual errors for CPT-11, SN-38 and SN-38G were lower in our model than in previously published models with proportional residual errors [12,20,21], denoting a better description of the data. The residual error for NPC was described with a combined error model and the constant part was 0.885 nmol. L^{-1}, close to the LOQ of NPC, which was 0. 964 nmol. L^{-1}.

The model developed here allowed us to test various covariates including the presence of oxaliplatin in the cancer treatment regimen. To our knowledge, no PK drug-drug interaction had been described so far between oxaliplatin and irinotecan [1,23]. Our study showed a significant impact of oxaliplatin ($p < 0.001$) on k_{43} value, corresponding to the first order rate constant from peripheral to central compartment of SN-38. Indeed, k_{43} mean value was 0.0132 h-1 in patients treated with FOLFIRI (n=84) versus 0.006 h-1 in patients treated with FOLFIRINOX (n=18). It can be concluded that oxaliplatin influences the distribution of SN-38. This could be explained by a direct or indirect competitive inhibition on ABC transporters, since both irinotecan and oxaliplatin are substrates of this transporters family [24,25], as has been previously described for paclitaxel and irinotecan [1,26].

In our study, the TATA box polymorphism on *UGT1A1*28* gene was studied as a covariate in the CPT-11 PopPK model for the first time. This covariate had a significant impact on k_{35} (constant rate of transformation from SN-38 to SN-38G), in accordance with pharmacogenetic knowledge [8].

Moreover, our model supported preceding results that gender [18,19], weight [19–21] and performance status [19] impact the PK of CPT-11 and its metabolites.

For comparison with findings of Mbatchi et al. on *NR1I2-rs10934498* polymorphism [13], the area under the curve (AUC) between 0 and 46 h was calculated for CPT-11 and its metabolites from the final model with covariates. Metabolic ratios of SN-38, SN-38G [13] and biliary index of Gupta [27] were calculated from AUC. AG and GG genotypes were grouped since the G allele of *NR1I2* is the dominant allele. In line with Mbatchi et al., we found only two statistically significant results: a decrease of SN-38 AUC (Wilcoxon, p=0.0069) and a decrease of biliary index of Gupta (p=0.0033) for the AA genotype. In addition, we compared individual PK parameters of the two genotype groups (AA vs AG/GG). While no clearance parameter appeared impacted by *NR1I2-rs10934498* polymorphism, the statistical analysis showed an increase of the volume of the central compartment for CPT-11, V_1 (t-test, p=0.02) and of the rate constant from central to peripheral compartment of SN-38, k_{34} (Wilcoxon p=0.011). These results confirm that *NR1I2-rs10934498* polymorphism influences the SN-38 PK, which could be ascribed to a regulation of ABC transporters [28].

The final model will be a useful tool to assess concentration-response relationships for CPT-11 and SN-38 and define target concentrations as a basis for therapeutic drug monitoring. In this context, the model will allow dosing individualization based on Bayesian estimation of individual parameters from sparse concentration measurements and to develop an optimized limited sampling strategy. Moreover, the current PK model will constitute the bedrock of future PK-PD models which are currently lacking and which are urgently needed to define optimal administration protocol, in order to reduce digestive toxicities of irinotecan while maintaining efficacy, in patients treated with FOLFIRI or FOLFIRINOX regimen for colorectal or pancreatic cancers.

Acknowledgements: The authors gratefully acknowledge Professor A. Iliadis for the assistance and the fruitful discussions regarding the model development. They would also like to thank the ligue Contre le Cancer French association who generously provided a PhD grant to Laure Deyme.

Conflict of Interest statement: Laure Deyme, Dominique Barbolosi, Litaty Céphanoée Mbatchi, Nicole Tubiana-Mathieu, Marc Ychou, Alexandre Evrard, and Florence Gattacceca declare that they have no conflict of interest.

Supplementary material: The model code that we developed is provided as an electronic supplementary information, so the model can be copy-pasted by any reader and run directly on Monolix® software with the users' own dataset. Additional GOF plots for CPT-11 and metabolites, including normalized prediction distribution errors, are provided in Supplementary File 2.

References

1. de Man FM, Goey AKL, van Schaik RHN, Mathijssen RHJ, Bins S. Individualization of Irinotecan Treatment: A Review of Pharmacokinetics, Pharmacodynamics, and Pharmacogenetics. Clin Pharmacokinet. 2018;57:1229-54.

2. Oyaga-Iriarte E, Insausti A, Sayar O, Aldaz A. Prediction of irinotecan toxicity in metastatic colorectal cancer patients based on machine learning models with pharmacokinetic parameters. J Pharmacol Sci. 2019;140:20-5.

3. Mathijssen RH, Van Alphen RJ, Verweij J, Loos WJ, Nooter K, Stoter G, et al. Clinical pharmacokinetics and metabolism of irinotecan (CPT-11). Clin Cancer Res. 2001;7:2182–2194.

4. Catimel G, Chabot GG, Guastalla JP, Dumortier A, Cote C, Engel C, et al. Phase I and pharmacokinetic study of irinotecan (CPT-11) administered daily for three consecutive days every three weeks in patients with advanced solid tumors. Ann Oncol. 1995;6:133-40.

5. Kehrer DFS, Yamamoto W, Verweij J, Jonge MJA de, Bruijn P de, Sparreboom A. Factors Involved in Prolongation of the Terminal Disposition Phase of SN-38: Clinical and Experimental Studies. Clin Cancer Res. 2000;6:3451-8.

6. Younis IR, Malone S, Friedman HS, Schaaf LJ, Petros WP. Enterohepatic recirculation model of irinotecan (CPT-11) and metabolite pharmacokinetics in patients with glioma. Cancer Chemother Pharmacol. 2009;63:517-24.

7. Loos WJ, Verweij J, Gelderblom HJ, de Jonge MJ, Brouwer E, Dallaire BK, et al. Role of erythrocytes and serum proteins in the kinetic profile of total 9-amino-20(S)-camptothecin in humans. Anticancer Drugs. 1999;10:705-10.

8. Rivory LP, Haaz MC, Canal P, Lokiec F, Armand JP, Robert J. Pharmacokinetic interrelationships of irinotecan (CPT-11) and its three major plasma metabolites in patients enrolled in phase I/II trials. Clin Cancer Res. 1997;3:1261-6.

9. Substances Irinotécan - VIDAL eVIDAL [Internet]. [cité 14 févr 2020]. Disponible sur: https://evidal-vidal-fr.ezproxy.uca.fr/substance/details/12311/irinotecan.html

10. Deyme L, Barbolosi D, Gattacceca F. Population pharmacokinetics of FOLFIRINOX: a review of studies and parameters. Cancer Chemother Pharmacol [Internet]. 2018 [cité 21 nov 2018]; Disponible sur: https://doi.org/10.1007/s00280-018-3722-5

11. Xie R, Mathijssen RHJ, Sparreboom A, Verweij J, Karlsson MO. Clinical pharmacokinetics of irinotecan and its metabolites in relation with diarrhea. Clin Pharmacol Ther. 2002;72:265-75.

12. Poujol S, Pinguet F, Ychou M, Abderrahim AG, Duffour J, Bressolle FMM. A limited sampling strategy to estimate the pharmacokinetic parameters of irinotecan and its active metabolite, SN-38, in patients with metastatic digestive cancer receiving the FOLFIRI regimen. Oncol Rep. 2007;18:1613-1321.

13. Mbatchi LC, Robert J, Ychou M, Boyer J-C, Del Rio M, Gassiot M, et al. Effect of Single Nucleotide Polymorphisms in the Xenobiotic-sensing Receptors NR1I2 and NR1I3 on the Pharmacokinetics and Toxicity of Irinotecan in Colorectal Cancer Patients. Clin Pharmacokinet. 2016;55:1145-57.

14. Poujol S, Pinguet F, Malosse F, Astre C, Ychou M, Culine S, et al. Sensitive HPLC-Fluorescence Method for Irinotecan and Four Major Metabolites in Human Plasma and Saliva: Application to Pharmacokinetic Studies. Clin Chem. 2003;49:1900-8.

15. Iliadis A. Structural identifiability and sensitivity. J Pharmacokinet Pharmacodyn. 2019;46:127-35.

16. Gabrielsson J, Weiner D. Enterohepatic recirculation. Pharmacokinetic and Pharmacodynamic Data Analysis: Concepts and Applications. Stockholm: Swedish Pharmaceutical Press. 2000.

17. Petricoul O, Claret L, Barbolosi D, Iliadas A, Puozzo C. Information Tools for Exploratory Data Analysis in Population Pharmacokinetics. J Pharmacokinet Pharmacodyn. 2001;28:577-99.

18. Berg AK, Buckner JC, Galanis E, Jaeckle KA, Ames MM, Reid JM. Quantification of the Impact of Enzyme-Inducing Antiepileptic Drugs on Irinotecan Pharmacokinetics and SN-38 Exposure. J Clin Pharmacol. 2015;55:1303-12.

19. Klein CE, Gupta E, Reid JM, Atherton PJ, Sloan JA, Pitot HC, et al. Population pharmacokinetic model for irinotecan and two of its metabolites, SN-38 and SN-38 glucuronide. Clin Pharmacol Ther. 2002;72:638-47.

20. Thompson PA, Gupta M, Rosner GL, Yu A, Barrett J, Bomgaars L, et al. Pharmacokinetics of irinotecan and its metabolites in pediatric cancer patients: a report from the children's oncology group. Cancer Chemother Pharmacol. 2008;62:1027-37.

21. Kimura T, Kashiwase S, Makimoto A, Kumagai M, Taga T, Ishida Y, et al. Pharmacokinetic and pharmacodynamic investigation of irinotecan hydrochloride in pediatric patients with recurrent or progressive solid tumors. Int J Clin Pharmacol Ther. 2010;48:327-34.

22. Mathijssen RHJ, Marsh S, Karlsson MO, Xie R, Baker SD, Verweij J, et al. Irinotecan Pathway Genotype Analysis to Predict Pharmacokinetics. Clin Cancer Res. 2003;9:3246-53.

23. Wasserman E, Cuvier C, Lokiec F, Goldwasser F, Kalla S, Méry-Mignard D, et al. Combination of oxaliplatin plus irinotecan in patients with gastrointestinal tumors: results of two independent phase I studies with pharmacokinetics. J Clin Oncol Off J Am Soc Clin Oncol. 1999;17:1751-9.

24. Biswas R, Bugde P, He J, Merien F, Lu J, Liu D-X, et al. Transport-Mediated Oxaliplatin Resistance Associated with Endogenous Overexpression of MRP2 in Caco-2 and PANC-1 Cells. Cancers [Internet]. 2019 [cité 4 juin 2020];11. Disponible sur: https://www.ncbi.nlm.nih.gov/pmc/articles/PMC6770320/

25. Ulrich CM, Robien K, McLeod HL. Cancer pharmacogenetics: polymorphisms, pathways and beyond. Nat Rev Cancer. Nature Publishing Group; 2003;3:912-20.

26. Asai G, Yamamoto N, Kurata T, Tamura K, Uejima H, Nakagawa K, et al. Phase I and Pharmacokinetic Study of Combination Chemotherapy Using Irinotecan and Paclitaxel in Patients with Lung Cancer. J Thorac Oncol. 2006;1:226-30.

27. Gupta E, Lestingi TM, Mick R, Ramirez J, Vokes EE, Ratain MJ. Metabolic Fate of Irinotecan in Humans: Correlation of Glucuronidation with Diarrhea. Cancer Res. American Association for Cancer Research; 1994;54:3723-5.

28. Ecker GF, Chiba P. Transporters as Drug Carriers: Structure, Function, Substrates. John Wiley & Sons; 2009.

Table Legends:

Table 1: Patient characteristics.

Values represent number of patients unless otherwise stated. **BSA:** body surface area; + **monoclonal Ab:** associated with monoclonal antibody; **UGT1A1*28:** TATA box polymorphism of the UGT1A1 promoter region; **NR1I2 – rs10934498:** NR1I2-rs10934498 polymorphism

Table 2: Population pharmacokinetic parameters of irinotecan and its four main metabolites from the 7-compartment model without and with covariates. Estimations from the data from 102 patients displaying UGT1A1 status.

$\mathbf{V_1}$**:** volume of the central compartment for CPT-11, $\mathbf{k_{12}}$: rate constant from central compartment of CPT-11 to peripheral compartment of CPT-11 ; $\mathbf{k_{21}}$: rate constant from peripheral compartment of CPT-11 to central compartment of CPT-11 ; $\mathbf{k_1}$: elimination rate of CPT-11, $\mathbf{k_{13}}$: metabolism rate of CPT-11 into SN-38, $\mathbf{k_{16}}$: metabolism rate of CPT-11 into APC; $\mathbf{k_e}$: combination of k_1, k_{13} and k_{16}; $\mathbf{V_{max}}$: maximum rate of metabolism of CPT-11 into NPC; $\mathbf{K_m}$: the half-saturating concentration of CPT-11 for metabolism of CPT-11 into NPC; $\mathbf{V_{3a}}$**:** apparent volume of the central compartment for SN-38, $\mathbf{k_{34}}$: rate constant from central compartment of SN-38 to peripheral compartment of SN-38; $\mathbf{k_{43}}$: rate constant from peripheral compartment of SN-38 to central compartment of SN-38 ; $\mathbf{k_{35}}$: metabolism rate of SN-38 into SN-38G; $\mathbf{V_{5a}}$: apparent volume of the central compartment for SN-38G; $\mathbf{k_5}$: elimination rate of SN-38G; $\mathbf{V_{6a}}$: apparent volume of the central compartment for APC; $\mathbf{k_6}$: elimination rate of APC; $\mathbf{V_7}$: Volume of the central compartment for NPC; **r**: ratio of metabolism rate of NPC into SN-38 on metabolism fraction of CPT-11 into SN-38; $\boldsymbol{\tau}$: delay; $\mathbf{k_7}$: elimination rate of NPC; $\beta_{parameter\_covariate}$: effect value of covariate on the parameter; ω: standard deviation of random effect; $\mathbf{b_1}$: proportional residual error for CPT-11; $\mathbf{b_3}$: proportional residual error for SN-38; $\mathbf{b_5}$: proportional residual error for SN-38G; $\mathbf{b_6}$: proportional residual error for APC; $\mathbf{a_7}$: constant residual error for NPC; $\mathbf{b_7}$: proportional residual error for NPC; *****: fixed value; **OFV**: objective function value; **-**: not included in the model

Figures:

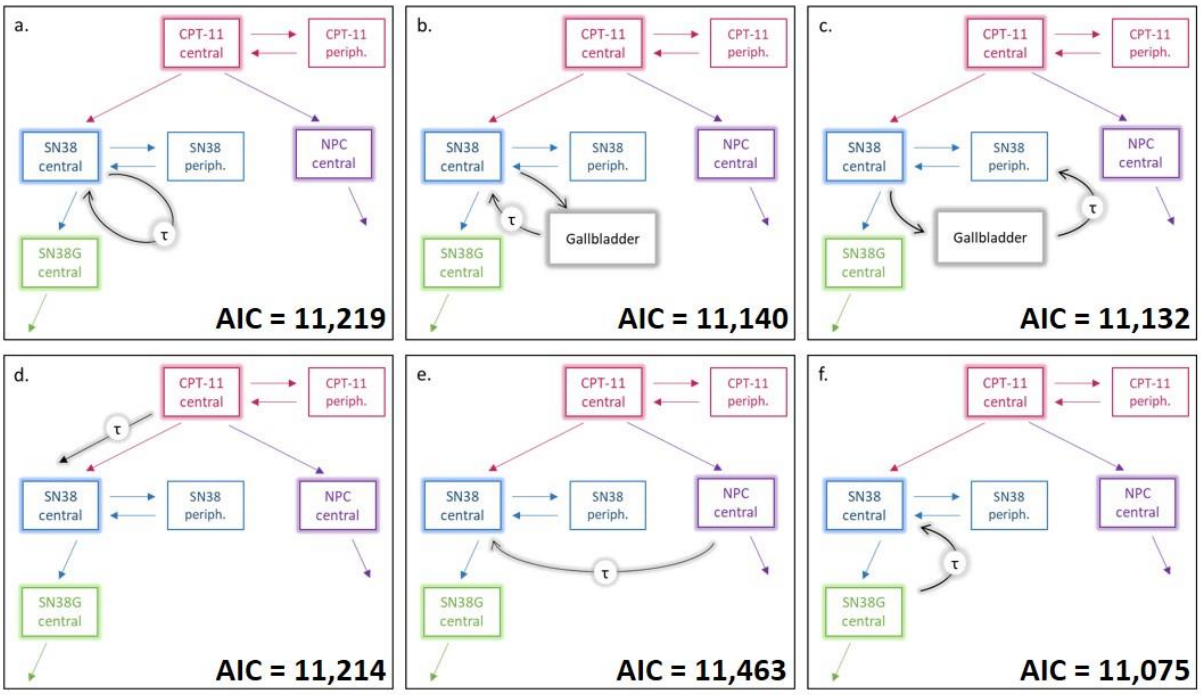

Fig. 1 Representation of the six models tested to describe the SN-38 rebound peak. AIC (Akaike Information Criteria) for estimations from 109 patients.

CPT-11 central: Central compartment of CPT-11; **CPT-11 periph**.: Peripheral compartment of CPT-11; **SN-38 central**: Central compartment of SN-38; **SN-38 periph**.: Peripheral compartment of SN-38; **SN-38G central**: Central compartment of SN-38G; **NPC central**: Central compartment of NPC; **Gallbladder:** gallbladder compartment; **τ**: delay

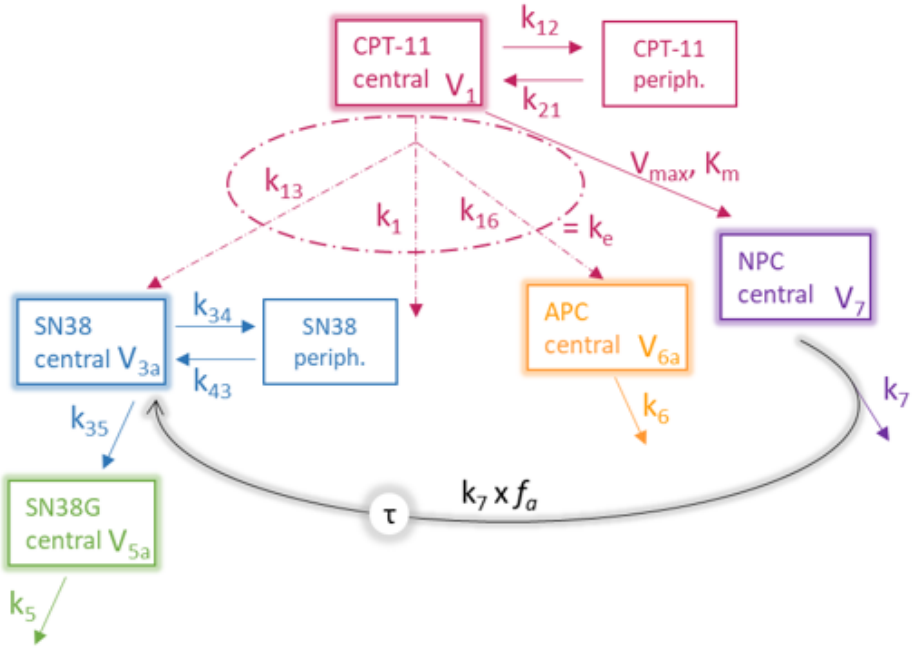

Fig. 2 Structural pharmacokinetic model for CPT-11 (1), SN-38 (3), SN-38G (5), APC (6) and NPC (7)

V_1: Volume of the central compartment for CPT-11, **k_{12}**: rate constant from central compartment of CPT-11 to peripheral compartment of CPT-11 ; **k_{21}**: rate constant from peripheral compartment of CPT-11 to central compartment of CPT-11 ; **k_1**: elimination rate of CPT-11, **k_{13}**: metabolism rate of CPT-11 into SN-38, **k_{16}**: metabolism rate of CPT-11 into APC; **k_e**: combination of k_1, k_{13} and k_{16}; **V_{max}**: maximum rate of metabolism of CPT-11 into NPC; **K_m**: the half-saturating concentration of CPT-11 for metabolism of CPT-11 into NPC; **V_{3a}:** Apparent volume of the central compartment for SN-38, **k_{34}**: rate constant from central compartment of SN-38 to peripheral compartment of SN-38; **k_{43}**: rate constant from peripheral compartment of SN-38 to central compartment of SN-38 ; **k_{35}**: metabolism rate of SN-38 into SN-38G; **V_{5a}**: apparent volume of the central compartment for SN-38G; **k_5**: elimination rate of SN-38G; **V_{6a}**: apparent volume of the central compartment for APC; **k_6**: elimination rate of APC; **V_7**: Volume of the central compartment for NPC; ***f_a***: the apparent metabolism rate of NPC into SN-38; **τ**: delay; **k_7**: elimination rate of NPC

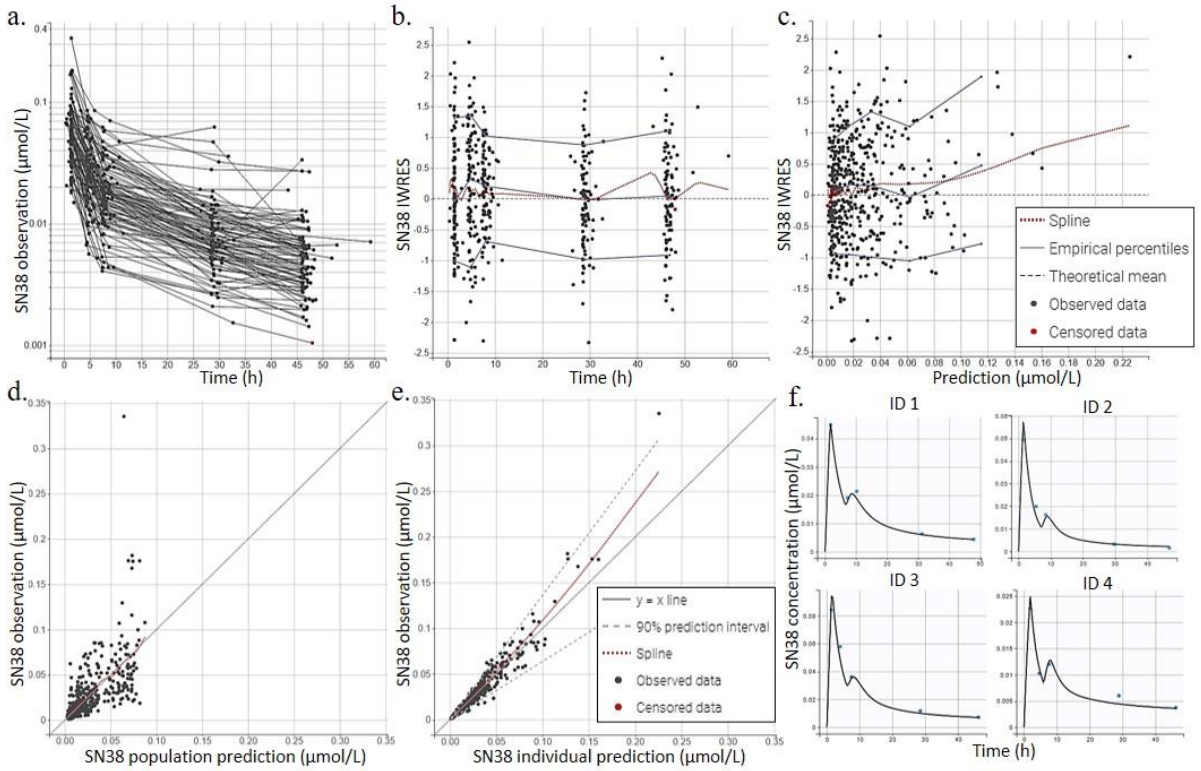

Fig. 3 Goodness-of-fit plots of the final model for SN-38

a. Observed data of SN-38. **b.** The individual weighted residuals (IWRES) of SN-38 versus predictions in µmol/L. **c.** IWRES of SN-38 versus time in hour. **d.** SN-38 observed concentration versus predicted population concentration. **e.** SN-38 observation versus predicted individual concentration. **f**. Four representative individual fits

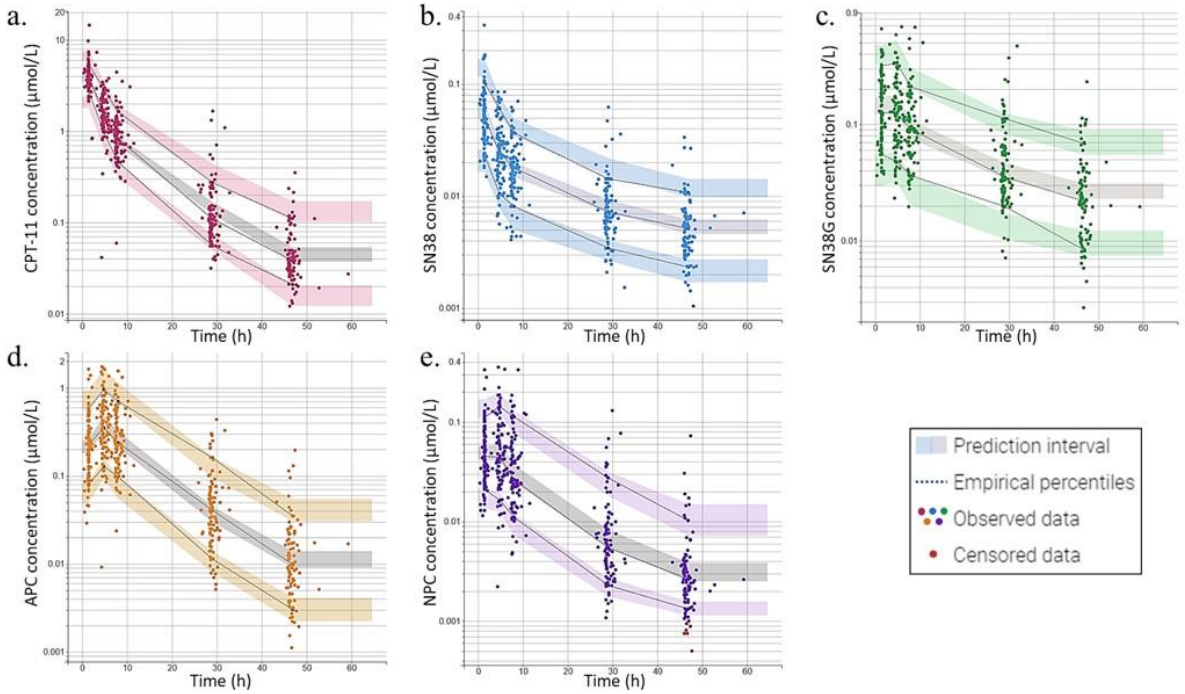

Fig. 4 Visual predictive checks for each molecule of the final model

a. CPT-11 ; **b**. SN-38 ; **c**. SN-38G ; **d**.APC ; **e**.NPC ; black circles : observed data ; grey circles : censored data ; dashed lines : 5th, 50th and 95th percentiles of the observed data ; shaded areas : 95%